LARGE TEMPERATURE ANISOTROPIES IN THE POLAR CORONAL HOLES: HOW RELIABLE ARE THEY?

N.-E. Raouafi[1] **and S. K. Solanki**[2]

[1]*National Solar Observatory, Tucson, Arizona, USA; E-mail: nraouafi@nso.edu*
[2]*Max-Planck-Institut für Sonnensystemforschung, Katlenburg-Lindau, Germany*

ABSTRACT

We examine the influence of different electron density stratifications on the coronal line-of-sight (LOS) integrated profiles of H I Ly-α and the O VI lines. We find that the widths of the O VI lines are significantly affected by the details of the adopted electron density profiles whereas Ly-α profiles are comparable to the observed ones for the different density models. Densities deduced from SOHO data result in O VI profiles whose widths and intensity ratio are relatively close to the values observed by UVCS although only isotropic kinetic temperatures are employed. Hence we expect the magnitude of the anisotropy to depend strongly on the density stratification adopted when analyzing the data.

Key words: Line: profiles – Scattering – Sun: corona – Magnetic fields – Sun: solar wind – Sun: UV radiation.

1. INTRODUCTION

Heavy ions in the polar coronal holes (i.e. O VI & Mg X) emit very broad lines in the extreme ultraviolet wavelength range. In order to reproduce the observed line widths, total intensities and intensity ratio of the O VI doublet, large anisotropies in the kinetic temperatures of these ions were invoked $\left(10 \leq T_{\perp}/T_{\parallel} \leq 100\right)$. These anisotropies are the results of an energy exchange between waves and ions at the cyclotron frequencies of the latter. According to this analysis, the energy exchange introduces huge anisotropies in the velocity turbulence of the different coronal species, which results in a consequent broadening the emitted line profiles.

In this paper, we present another simpler interpretation of the observations. We consider the influence of the density stratification details on the LOS-integrated profiles. The importance of the density stratification resides in the fact that it influences directly the outflow speed of the ions through the mass-flux conservation equation in addition to the effect of the absolute density number on the intensity of the spectral lines. We compute the intensity profiles of H I Ly-α and O VI doublet. We take into account the effect of the solar wind (Doppler dimming and the optical pumping of the O VI $\lambda 1037.6$ line by the chromospheric C II doublet). Only simple Maxwellian velocity distributions characterized by mean velocity, $\boldsymbol{V}$, and velocity turbulence, α_S, are considered. No anisotropy in the velocity turbulence is considered.

2. MODEL: ELECTRON DENSITY, CORONAL MAGNETIC FIELD AND SOLAR WIND

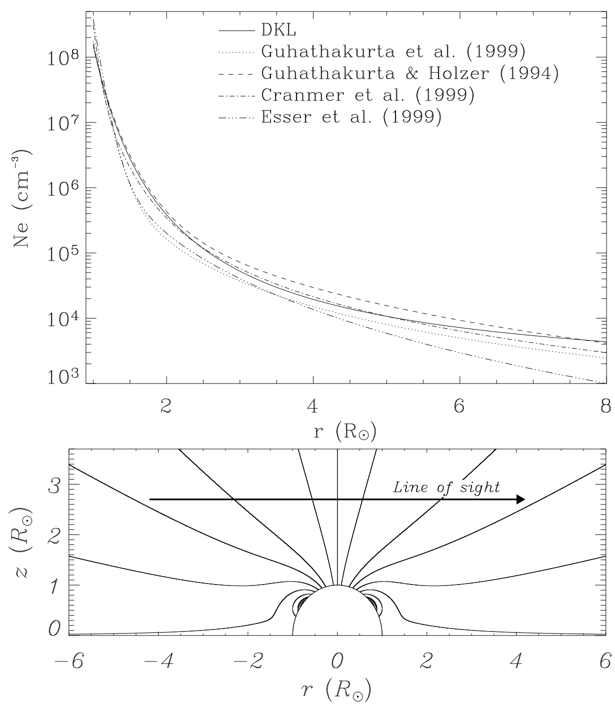

Figure 1. Top: electron density stratifications for different empirical models used for the computation of EUV lines. Bottom: large scale magnetic field of the corona at the solar activity minimum according to the model by Banaszkiewicz et al. (1998). A sample of the LOS is indicated by the horizontal arrow.

We consider different empirical density models for the polar coronal holes taken from different sources (top

Proc. SOHO 17 – 10 Years of SOHO and Beyond, Giardini Naxos, Sicily, Italy
7 – 12 May 2006 (ESA SP-617, July 2006)

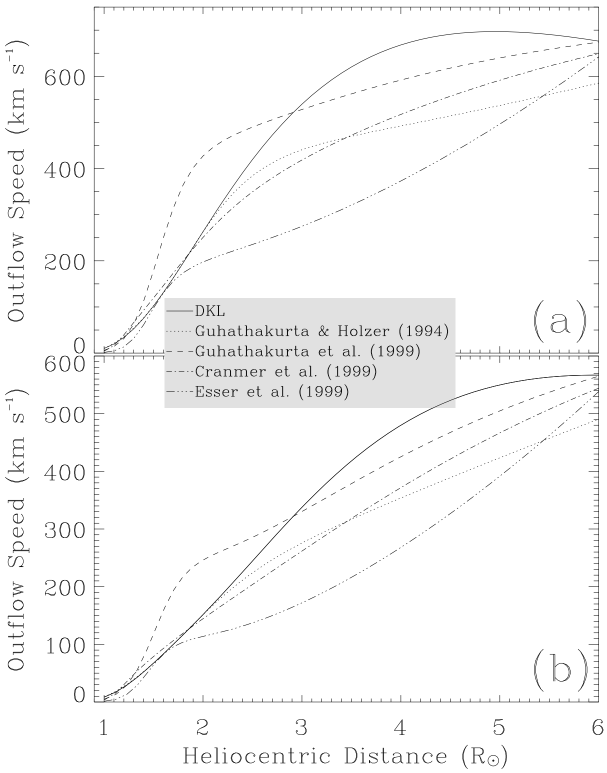

Figure 2. Outflow speed of the O VI *ions along the polar axis* (a) *and field line arising from 70 degree latitude* (b)*, respectively, for the different density models considered.*

panel of Figure 1). The DKL density stratification is obtained from SOHO data (SUMER, UVCS and LASCO; see Doyle et al. 1999). As shown by Figure 1, the absolute density numbers as a function of height are comparable for the different models although small differences are noticeable. We expect the latter to significantly affect the LOS-integrated profiles. The large scale coronal magnetic field is given by the model of Banaszkiewicz et al. (1998; bottom panel of Figure 1). This model is based on the distribution of coronal structures and represents fairly well the corona during the minimum of the solar activity cycle.

Using the field model and the different density stratifications, the outflow speed of the different coronal species is obtained through the mass flux conservation equation. The outflow speed of the ions at the coronal boundary is chosen to be proportional to the solar surface magnetic field strength. However, this dependence is rather small. In order to get as close as possible to the measured profiles, we adopt different values of the proportionality coefficient of $V(R_\odot, \theta_\odot)^1$ with respect to $B(R_\odot, \theta_\odot)$ for the different density models. A further constraint on the wind speed is that it should reach values between 600-700 km s^{-1} above $6.0 - 7.0\ R_\odot$ (see Figure 2).

The range of integration along the LOS is also an important factor in particular at high altitudes. In fact, at low heights the density drop is very rapid and then the main contribution comes from a small range along the LOS (about $1.0 - 2.0\ R_\odot$ around the polar axis). However, higher up the density decrease is slower and then significant contributions to the line profile come from further sections along the LOS. This is shown clearly by Figure 3 in Raouafi & Solanki (2006; hereafter referred to as RS06).

[1] $\theta_\odot$ is the latitude angle on the solar disk

3. RESULTS

Ly-α is formed by the resonant scattering of the solar disk radiation (electron collisions are negligible). The O VI lines are excited by both, the radiation coming from the transition region and by electron collisions. We assume that α_S depends only on r, so that its value changes along the LOS. In the next sections, we describe the profile calculations of these two sets of lines and their comparison with the observed ones.

3.1. H I Ly-α

The incident solar disk Ly-α profile is fitted by four Gaussians plus a constant background (see Figure 6 in RS06). Numerically, we assume that coronal hydrogen atoms are illuminated by the photons of four incident Gaussian profiles emitted by the solar disk, with of course different parameters (Table 3 in RS06). No center-to-limb variation in the intensity emitted by the solar disk is considered (Bonnet et al. 1980).

A single Gaussian is sufficient to fit the calculated off-limb Ly-α profiles with good accuracy. The top panel of Figure 3 displays the e-folding (Doppler) widths of the computed Ly-α profiles as a function of height. The synthetic Ly-α profiles are relatively in-sensitive to the details of the electron density stratification. For most of the density stratifications given in Figure 1, the observed line width of Ly-α at different heights in the polar coronal holes are comparable to the calculated ones in the presence of an isotropic turbulence velocity α_S displaying a gradual rise with height. The displayed results are all located in the 1-σ error bars of measured widths except for the widths obtained at low altitudes by using densities given by Guhathakurta et al. (1999) or between 2.3 and 2.7 $R_\odot$ based on the Esser et al. (1999) densities. The reasons for these departures are visible in Figure 2; note the high/low outflow speeds obtained through these density models at these altitudes. The bottom panel of Figure 3 displays the total intensities of Ly-α as a function of height for the different density stratifications considered. All the density models considered give total intensities that are close to the observed ones (within a factor of 2-3). For more details, see RS06.

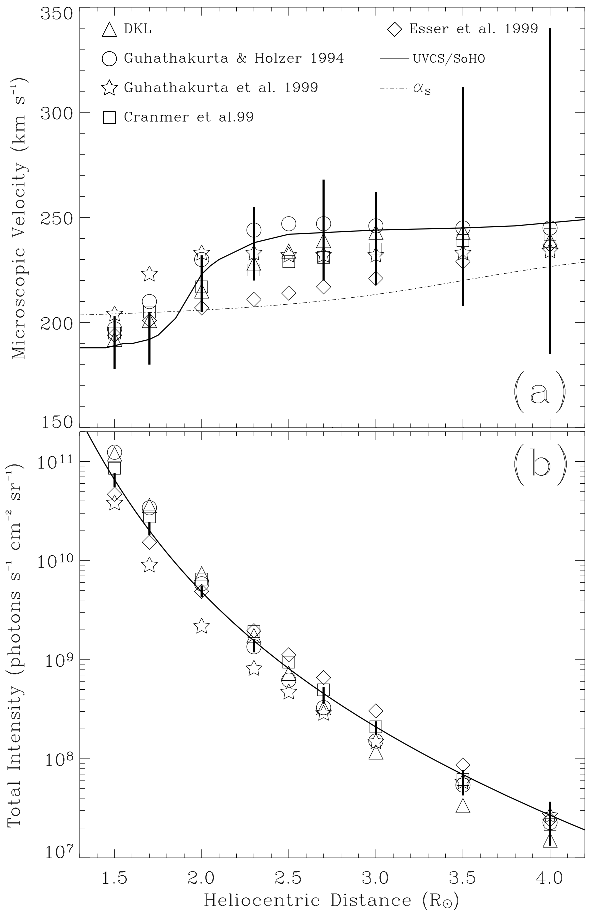

Figure 3. Widths (a) *and total intensities* (b) *of the computed LOS-integrated Ly-α line profile as a function of height obtained for the different density models (Figure 1). The correspondence of symbols to density models is given in the top panel. The solid lines are the best fits to UVCS observations (Cranmer et al. 1999) and the dot-dashed line (top panel) is the velocity turbulence, α_S, of the hydrogen atoms. The vertical lines are the statistical error bars of the measurements.*

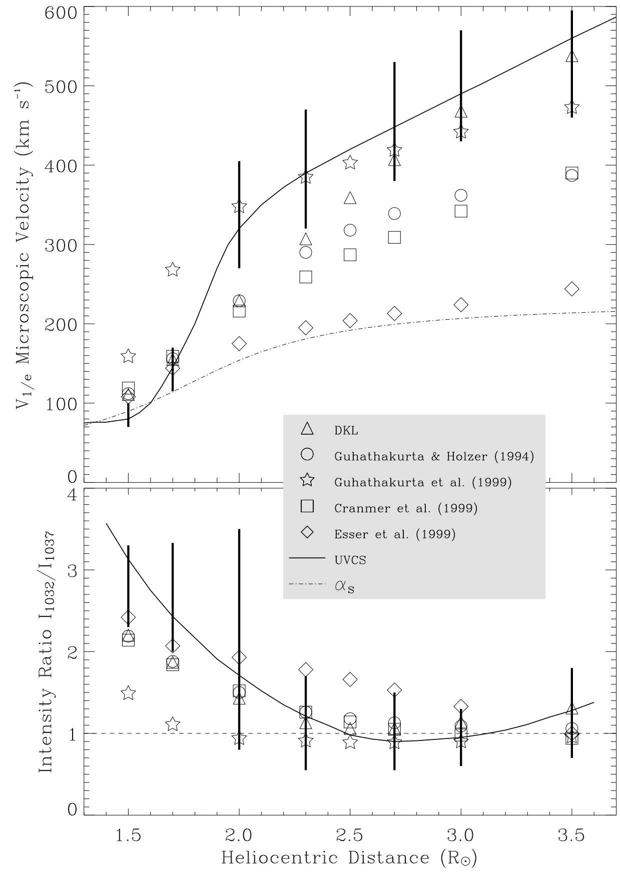

Figure 4. Widths (top) and intensity ratio (bottom) of the LOS-integrated profiles of O VI *as a function of altitude. The dot-dashed curve in the top panel displays the used values of α_S. The correspondence between symbols and density models is indicated in the gray frame. The observed dependence is given by the solid curves (best fits to the observations; see Cranmer et al. 1999), with the vertical lines being error bars.*

3.2. O VI lines

The intensity profiles of the O VI doublet (103.2 nm and 103.7 nm) are computed for the different density models considered. The effects of the ions' motion are taken into account via the Doppler dimming, the Doppler shift and the optical pumping of the O VI 103.7 nm line by the chromospheric C II doublet. Details of the parameters are given in RS04 ande RS06 and references therein.

The top panel of Figure 4 displays the widths of the calculated O VI 103.2 nm line as a function of altitude and for the different density stratifications. These widths are obtained by applying a Gaussian fit to each calculated profile. All profiles are well represented by one Gaussian. The profiles at the furthest considered ray (3.5 $R_\odot$) show the strongest departure from a Gaussian shape (see Figure 10 of RS06). The solid line represents the best fit to the UVCS data (Cranmer et al. 1999). Note that no anisotropy in the kinetic temperature of the emitting ions is considered.

At small heights ($< 2.0\ R_\odot$) the widths of the calculated profile are comparable for most of the density models except for the one by Guhathakurta et al. (1999). For this model the boundary condition on the solar wind speed at the solar surface is chosen to fit the widths at high latitudes. This gives high solar wind speeds already at 1.5 $R_\odot$ and explains the broader profiles resulting from this model at low altitudes. At larger heights ($> 2.0\ R_\odot$) the line widths are very sensitive to the details of the electron density stratification. This can be easily seen by the difference in the widths of the different profiles obtained through slightly different density stratification models. The DKL model gives line widths comparable to the ones obtained from the data, except between 2.0 and 2.3 $R_\odot$, where the obtained widths are slightly smaller than the observed ones.

The bottom panel of Figure 4 displays the ratio of total intensities of the O VI doublet lines as a function of

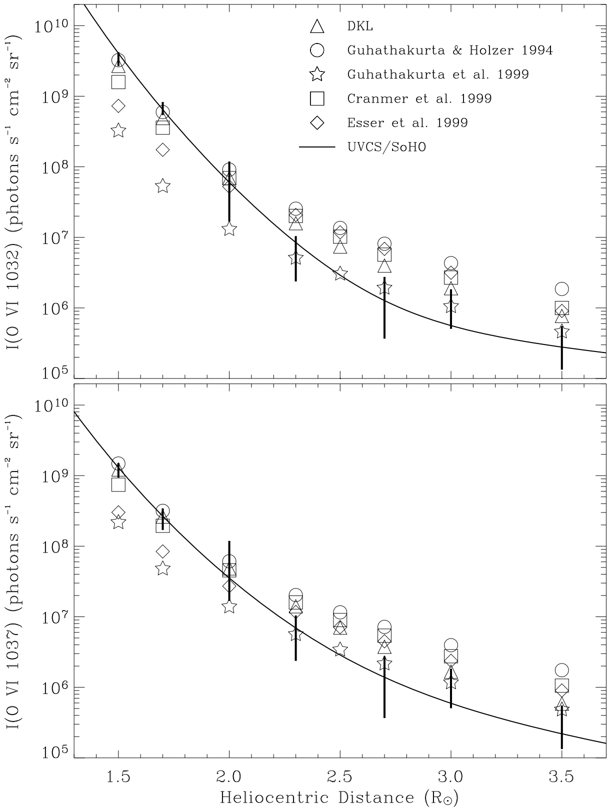

Figure 5. Total intensities of the O VI *lines as a function of altitude. The correspondence to the different density stratifications is given by the symbols in the top panel. The solid curves are the best fits to the observed intensities by UVCS and the vertical bars represent estimates of the accuracy of the observations.*

height. This ratio exhibits a marked dependence on radial distance, being well over 2 close to the Sun, then dropping rapidly. The exception is the density models by Esser et al. 1999, which produces larger ratios than the other density models and which do not fit the observations in particular at distances between 2.3 and 3 $R_{\odot}$). All the other models lead to a minimum in the ratio at $r \approx 2.5 - 3.0\ R_{\odot}$, which then increases again at larger r (a number of the considered models exhibit a slightly different behavior, showing a slight decrease in the ratio out to r = 3.5 $R_{\odot}$). Generally, most of the calculated intensity ratios (in particular those obtained from the DKL density stratification) are within the error bars of the ones observed by UVCS.

Figure 5 displays the computed total intensities of the O VI lines as a function of height. The density model of DKL, Cranmer et al., Guhathakurta & Holzer, and for $r \geq 2.0\ R_{\odot}$, Esser et al. give comparable intensities of the O VI doublet that agree reasonably with the observations. All models produce a slightly less steep drop in intensity with altitude than suggested by the observations, however. The density models by Guhathakurta et al. (1999) and Esser et al. (1999) give low intensities at low altitudes. This is due the fast drop of the electron density at low altitudes for these two models.

4. CONCLUSIONS

Although no anisotropy is considered in the kinetic temperature of coronal species, we find that

- Ly-α profiles obtained from different density stratifications are comparable and reasonably fit the observed ones
- O VI profiles depend strongly on the details of density stratification
- The O VI widths, total intensities and intensity ratios obtained from the DKL density model are comparable to the observed ones
- Difference in the kinetic temperatures of heavy ions and protons found in earlier works is present in our analysis. This is all the more surprising since we did not in any way optimize the computations with such an aim.
- Our analysis suggests that the need for coronal kinetic temperature anisotropies may not be so pressing as previously concluded, although we stress that the current results do not rule out such anisotropies.

For more details, see Raouafi & Solanki (2004 & 2006).

REFERENCES

Banaszkiewicz, M., Axford, W. I., & McKenzie, J. F. 1998, A&A, 337, 940

Bonnet, R. M., Decaudin, M., Bruner, E. C., Jr., Acton, L. W., & Brown, W. A 1980, ApJ, 237, L47

Cranmer, S. R., Kohl, J. L., Noci, G., et al. 1999, ApJ, 511, 481

Doyle, J. G., Teriaca, L., & Banerjee, D. 1999, A&A, 349, 956

Esser, R., Fineschi, S., Dobrzycka, D., et al. 1999, ApJ, 510, L63

Guhathakurta, M., & Holzer, T. E. 1994, ApJ, 426, 782

Guhathakurta, M., et al. 1999, JGR, 104, 9801

Raouafi, N.-E. & Solanki, S. K. 2004, A&A, 427, 725

Raouafi, N.-E. & Solanki, S. K. 2006, A&A, 445, 735